CrystEngComm

Accepted Manuscript

ROYAL SOCIETY OF CHEMISTRY

www.rsc.org/crystengcomm

Cite this: DOI: 10.1039/c0xx00000x

www.rsc.org/xxxxxx

ARTICLE TYPE

Melting point–solubility–structure correlations in multicomponent crystals containing fumaric or adipic acid

Eustina Batisai, Alban Ayamine, Ornella E. Y. Kilinkissa and Nikoletta B. Báthori*

Received (in XXX, XXX) Xth XXXXXXXXX 20XX, Accepted Xth XXXXXXXXX 20XX

DOI: 10.1039/b000000x

This study investigates the relationships between the supramolecular structure and the solubility and melting point of six multicomponent crystals involving fumaric acid (FUM series) and adipic acid (ADI series). The crystals were prepared by solvent evaporation and fully characterised by thermal and diffraction techniques. In each series the melting points of the multicomponent crystals are lower than the relevant carboxylic acid and they show partial correlation with their aqueous solubilities. With the aid of Hirshfeld surface analysis, the relationships between solubility, melting point and the supramolecular structure are discussed.

Introduction

The cocrystallisation approach has recently found application in the preparation of pharmaceutical cocrystals[1,2,3] with improved physicochemical properties, eg solubility[4,5,6,7] and stability.[8] Solubility is an important property as it can affect the dissolution rate and consequently bioavailability.[9] Based on the biopharmaceutics classification system (BCS), approximately 40% of drugs on the market are categorized as Class II and IV, which represent drugs with low solubility.[10]

The relationship between the supramolecular structure of a drug and some of its physicochemical properties such as solubility and melting point forms an important part of pharmaceutical research. The melting point is a fundamental property that has found utility in the estimation of vapour pressure, boiling point and aqueous solubility.[11] While the melting point is an easily measurable property, solubility determination is time consuming and tedious. An estimate of the solubility of a drug before it is synthesised could be helpful not only in terms of saving costs and time but also in designing combinatorial libraries for drug discovery.[12] For these reasons, several computational methods have been developed for estimating solubility from the drug chemical structure[12,13,14,15] or from the experimentally determined melting point[16,11] with varying success. It has thereby been established that the aqueous solubility of a compound can be quantitatively related to its melting point and partition coefficient.[17] In cocrystals, where two or more compounds exist in the crystal lattice, melting point correlations to solubility or their utility in solubility estimation is still a challenge.[1,18] However, it has been shown that properties of pharmaceutical cocrystals can be tuned by judicious selection of the coformer. For example, if one wishes to increase the thermal stability of a given active pharmaceutical ingredient, then a coformer with a higher melting point is used. Indeed, studies by Aakeröy in 2009[19] and more recently in 2014[4] have shown that the melting points of pharmaceutical cocrystals can be controlled in a systematic manner by cocrystallisation with a series of structurally related coformers. Even though good correlation between melting points of cocrystals and their coformer was reported, no correlation was found between coformer solubility and cocrystal solubility. In another study, direct proportionality between cocrystal solubility and coformer solubility was reported in a series of salicylic acid cocrystals.[20]

As part of our ongoing interest in investigating the structure-property relationships in cocrystals we have prepared four structurally related novel solvates of fumaric acid (**FUM**) and adipic acid (**ADI**) with 3-picoline (**3PIC**) and 4-picoline (**4PIC**); $C_4H_4O_4{\cdot}2(C_6H_7N)$ (**FUM3PIC** and **FUM4PIC**) and $C_6H_{10}O_4{\cdot}2(C_6H_7N)$ (**ADI3PIC** and **ADI4PIC**) (Scheme 1).

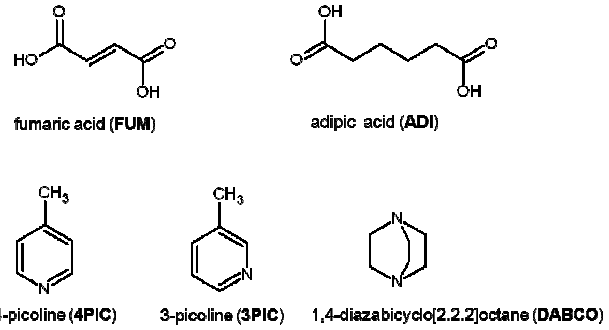

Scheme 1 The structures and abbreviations of compounds used in this study

The aim of this study was to establish a correlation between the melting point and the solubility, if any, and to investigate how these physicochemical properties relate to the supramolecular structure. The choice of the dicarboxylic acids and picolines was influenced by their simplicity and also because they possess hydrogen bonding groups capable of forming the reliable $COOH{\bullet\bullet\bullet}N_{aromatic}$ heterosynthon. Although these compounds are

not pharmaceutical cocrystals they are in fact model cocrystals which represent the same types of motifs that are present in some drugs and pharmaceutical cocrystals. We have also reproduced the two previously reported salts of 1,4-diazabicyclo[2.2.2]octane (**DABCO**) with fumaric acid, $2[C_4H_3O_4^-][C_6H_{14}N_2^{2+}]$ and adipic acid, $[C_6H_9O_4^-][C_6H_{13}N_2^+]$ hereafter referred to as **FUMDABCO** and **ADIDABCO** respectively. [21,22,23] Guided by the quantitated pKa rule by Cruz-Cabeza,[24] we expected salt formation for structures **FUM3PIC** (ΔpKa = 2.08),[25] **FUM4PIC** (ΔpKa = 2.30), **ADI3PIC** (ΔpKa = 1.71) and **ADI4PIC** (ΔpKa = 1.93) since in this ΔpKa range (1.71-2.30) the probability of salt formation is 60-70%. However, we did not observe any proton transfer in these structures.[26,27,28] **FUMDABCO** and **ADIDABCO** were chosen as part of this study because these two structures contain the same dicarboxylic acids and consist of charge assisted hydrogen bonds. The crystal structures of the four solvates as well as the two salts were analysed by single crystal X-ray diffraction (SCXRD) and melting points were measured using differential scanning calorimetry (DSC). Solubilities were determined in water and ethanol. Typically, drug solubility is measured in water, ethanol and octanol because this would give an indication of the behaviour of the drug in the polar, intermediate and non-polar environments in biological systems.[29] In addition, aqueous and ethanol solubilities are important as water and ethanol are the media commonly used for drug delivery.[29] With the aid of Hirshfeld surface analysis[30,31] an attempt was made to discuss the relationship between the supramolecular structure, melting point and solubility.

Experimental

All chemicals were purchased from Sigma Aldrich and used without further purification. Single crystals of **FUM3PIC**, **FUM4PIC**, **ADI3PIC** and **ADI4PIC** were prepared by dissolving each dicarboxylic acid in 3- and 4-picoline in separate experiments and allowing the solvent to evaporate slowly. **FUMDABCO** and **ADIDABCO** were prepared following the reported procedures.[21,22,23] In all cases, colourless block shaped crystals were obtained after a few days. DSC was carried out using a Perkin Elmer 6 under a N_2 gas purge (flow rate of 30.0 ml/min). Experiments were conducted over a temperature range of 30 °C to 350 °C. Powder X-ray diffraction (PXRD) data were recorded on a Bruker D2 phaser diffractometer using CuKα radiation (1.54184 Å) generated at 30 kV and 10 mA. Simulated powder patterns of crystal structures were calculated using Mercury[32] and compared with the experimental patterns to confirm bulk phase purity (Fig. S1-S4). Equilibrium solubility values were determined in both water and ethanol at 25 °C using the gravimetric method (Fig. S5 and S6).

X-ray crystallography

Intensity data for **ADI3PIC** and **FUM3PIC** were collected on a Nonius Kappa CCD single crystal X-ray diffractometer using graphite monochromated MoKα radiation (λ = 0.7107 Å, T = 173 K) generated by a Nonius FR590 generator at 50 kV and 30 mV. A series of frames were recorded, each of width 1° in ø or in ω to ensure completeness of the data collected to θ > 28°. The unit cell was indexed from the first ten frames, and positional data were refined along with diffractometer constants to give the final cell parameters. The strategy for data collection was evaluated using COLLECT[33] software. Integration and scaling (DENZO and SCALEPACK)[34] resulted in unique data sets corrected for Lorentz polarization effects and for the effects of crystal decay and absorption by a combination of averaging of equivalent reflections and overall volume and scaling correction. Intensity data for **FUM4PIC** and **ADI4PIC** were collected on the Bruker DUO APEX II diffractometer[35] with graphite-monochromated MoKα radiation (λ = 0.71073 Å) at 173K using an Oxford Cryostream 700. Data collection and cell refinement were performed using *SAINT-Plus*[36] and the space groups were determined from systematic absences using *XPREP*[37] and further justified by the refinement results. Accurate unit cell parameters were refined on all data. The structures were solved using *SHELXS-97*[38] and refined using full-matrix least squares methods in *SHELXL-97*,[38] within the X-Seed[39] graphical user interface. Non-hydrogen atoms were refined anisotropically and hydroxyl hydrogen atoms were located in the difference electron density map. The hydrogen atoms bound to carbon atoms were placed at idealized positions and refined as riding atoms. For the **ADI4PIC** structure E-statistics indicated a *P*-1 space group but upon refinement, the methyl groups of the picoline showed disorder. We therefore refined the structure in *P*1 and, interestingly, the hydrogen atoms of the methyl groups showed no disorder and were not related by the pseudo centre of symmetry located at the centre of the **ADI** methylene chain. Thus this structure is non-centrosymmetric only by virtue of the different orientation of the methyl hydrogen atoms of the picoline. Crystal data and hydrogen bond details are given in Table 1 and Table 2 respectively. CCDC deposit numbers 1008278-1008281 contains the supplementary crystallographic data for this paper. These data can be obtained free of charge from the Cambridge Crystallographic Data Centre via www.ccdc.cam.ac.uk/ data_request/cif.

Grinding experiments

In order to determine whether the solvates **FUM3PIC**, **FUM4PIC**, **ADI3PIC** and **ADI4PIC** can be obtained mechanochemically, the starting materials were ground with a mortar and pestle for thirty minutes and the resulting compounds were analysed by PXRD. The PXRD patterns show that **FUM4PIC** and **ADI3PIC** can be reproduced by grinding while a different phase of **FUM3PIC** is produced. Grinding also produces the same phase of **ADI4PIC** as solution synthesis but with some traces of unreacted adipic acid (see ESI Fig. S1-S4).

Results and discussion

Crystals of **FUM3PIC**, **FUM4PIC**, **ADI3PIC** and **ADI4PIC** suitable for SCXRD were prepared by the solvent evaporation technique. Except for **ADI4PIC**, the asymmetric units consist of one molecule of 3- or 4-picoline and half a molecule of a dicarboxylic acid located on an inversion centre (Fig. 1(a-c)). The asymmetric unit of **ADI4PIC** consists of one molecule of adipic acid and two molecules of 4-picoline (Fig. 1(d)). In all four structures, the molecules are linked into discrete units via carboxylic acid•••picolinyl interactions involving a strong O-H•••N hydrogen bond and an additional weaker C–H•••O

Table 1 Selected crystal data, experimental and refinement parameters for structures **FUM3PIC, FUM4PIC, ADI3PIC** and **ADI4PIC**

	FUM3PIC	**FUM4PIC**	**ADI3PIC**	**ADI4PIC**
CCDC number	1008280	1008279	1008278	1008281
Molecular formula	$C_{16}H_{18}N_2O_4$	$C_{16}H_{18}N_2O_4$	$C_{18}H_{24}N_2O_4$	$C_{18}H_{24}N_2O_4$
Formula weight	302.32	302.32	332.39	332.39
Temperature (K)	173(2)	173(2)	173(2)	173(2)
Crystal system	monoclinic	monoclinic	monoclinic	triclinic
Space group	$P2_1/c$	$P2_1/c$	$P2_1/n$	$P1$
a/Å	9.805(2)	8.746(2)	5.473(1)	6.948(1)
b/Å	4.810(1)	7.217(1)	14.309(3)	7.162(1)
c/Å	16.660(3)	12.799(3)	11.659(2)	10.509(2)
α/°	90	90	90	78.17(3)
β/°	98.91(3)	92.68(3)	99.48(3)	73.90(1)
γ/°	90	90	90	62.48(3)
Volume (Å^3)	776.2(3)	807.0(3)	900.6(3)	443.8(2)
Z	2	2	2	1
ρ (g cm^{-3})	1.294	1.244	1.226	1.244
μ (mm^{-1})	0.094	0.090	0.087	0.088
Limiting indices (*hkl*)	±13; ±16; ±22	±11; ±9; -17, 16	±13; ±6; ±22	±9; ±9; ±13
Reflections collected/unique	3742/2005	6600/2015	4023/2051	8165/2207
R_{int}	0.0216	0.0325	0.0372	0.0215
Final R indices [$I > 2\sigma(I)$]	$R_1 = 0.0382$; w$R_2 = 0.1054$	$R_1 = 0.0409$; w$R_2 = 0.1048$	$R_1 = 0.0461$; w$R_2 = 0.1160$	$R_1 = 0.0364$; w$R_2 = 0.1037$

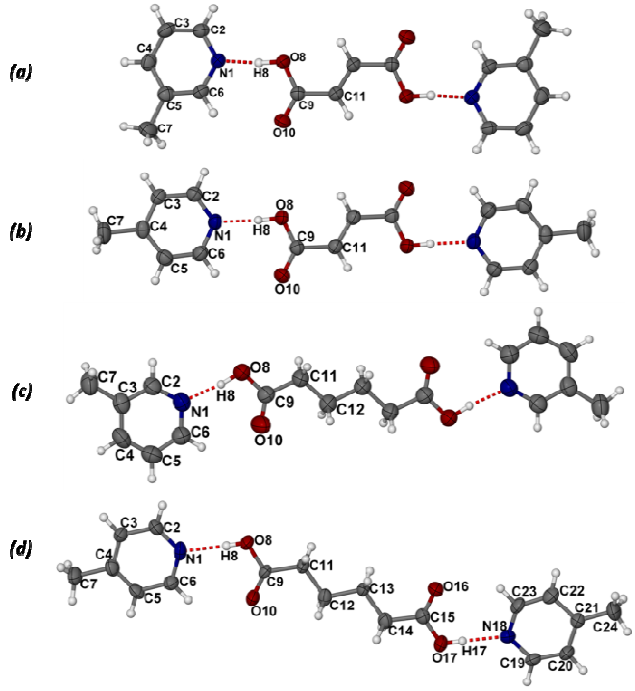

Fig. 1 (a-d) The molecular structure of **FUM3PIC**, **FUM4PIC**, **ADI3PIC** and **ADI4PIC** respectively showing thermal ellipsoids at 70% probability level for non-hydrogen atoms

Table 2 Hydrogen bond details and short contacts

D−H•••A	D−H (Å)	H•••A (Å)	D•••A (Å)	∠D−H•••A (°)
FUM3PIC				
O8−H8•••N1	0.97	1.63	2.595(1)	173.7
C6−H6•••O 0	0.95	2.68	3.351(1)	127.8
C2−H2•••O8^{i}	0.95	2.55	3.240(2)	129.9
FUM4PIC				
O8−H8•••N1	0.91	1.68	2.583(1)	170.1
C6−H6•••O10	0.95	2.61	3.275(2)	127.6
C2−H2•••O8^{ii}	0.95	2.54	3.239(2)	130.8
C7−H7C•••O10^{iii}	0.98	2.63	3.590(2)	166.0
ADI3PIC				
O8−H8•••N1	0.95	1.71	2.664(2)	176.4
C6−H6•••O10	0.95	2.51	3.208(2)	130.6
C4−H4•••O10^{iv}	0.95	2.43	3.340(2)	161.0
ADI4PIC				
O8−H8•••N1	0.90	1.79	2.688(4)	176.2
O17−H17•••N18	0.92	1.76	2.684(5)	173.6
C6−H6•••O10	0.95	2.55	3.261(6)	132.1
C23−H23•••O16	0.95	2.59	3.285(6)	130.5
C2−H2•••O17^{v}	0.95	2.57	3.376(5)	142.9
C19−H19•••O8^{vi}	0.95	2.56	3.370(4)	143.6
C5−H5•••O16^{vii}	0.95	2.43	3.307(5)	153.6
C22−H22•••O10^{viii}	0.95	2.43	3.317(6)	154.5

Symmetry codes: (i) –x+2, y-1/2, -z+3/2, (ii) -x+1, y-1/2, -z+1/2, (iii) x, -y+1/2, z-1/2, (iv) -x+3/2, y+1/2, -z+3/2, (v) x-1, y, z-1, (vi) x+1, y, z+1, (vii) x-1, y-1, z and (viii) x+1, y+1, z

interaction between the ortho hydrogen and the carbonyl moiety. In the **FUM3PIC** structure the hydrogen bonded units pack in layers along the *b* axis, and the entities in consecutive layers interact with each other via a weak interaction involving the hydroxyl oxygen and one of the picolinyl hydrogen atoms (C2–H2•••O8; 3.240(2) Å; 129.9°) (Fig. 2(a)). Units in the same layers interact with each other via π•••π interactions of 3.29 Å between the picolinyl moiety and the carboxylic group (C6•••C9). The **FUM4PIC** structure also consists of layers along the *b* axis and the hydrogen bonded units interact with those in consecutive layers via three short contacts (C2–H2•••O8; 3.239(2) Å; 130.8° and C7– H7C•••O10; 3.590(2) Å; 166.0° and H5•••H5 = 2.33 Å) as well an interaction between the picolinyl moiety and one of the hydrogen atoms of the methyl group (C7–H7C•••π = 3.45 Å). In the **ADI3PIC** structure the units are arranged in a herringbone fashion along the *c* axis and they interact with each other via two short contacts (C4–H4•••O10; 3.340(2) Å; 161.0° and H6•••H7A = 2.31 Å) to form 2D sheets (Fig. 2(c)).These sheets pack on top of each other and interact via two C–H•••π interactions (C12–H12A•••π =2.98 Å and C13–H13B•••π = 3.69 Å).

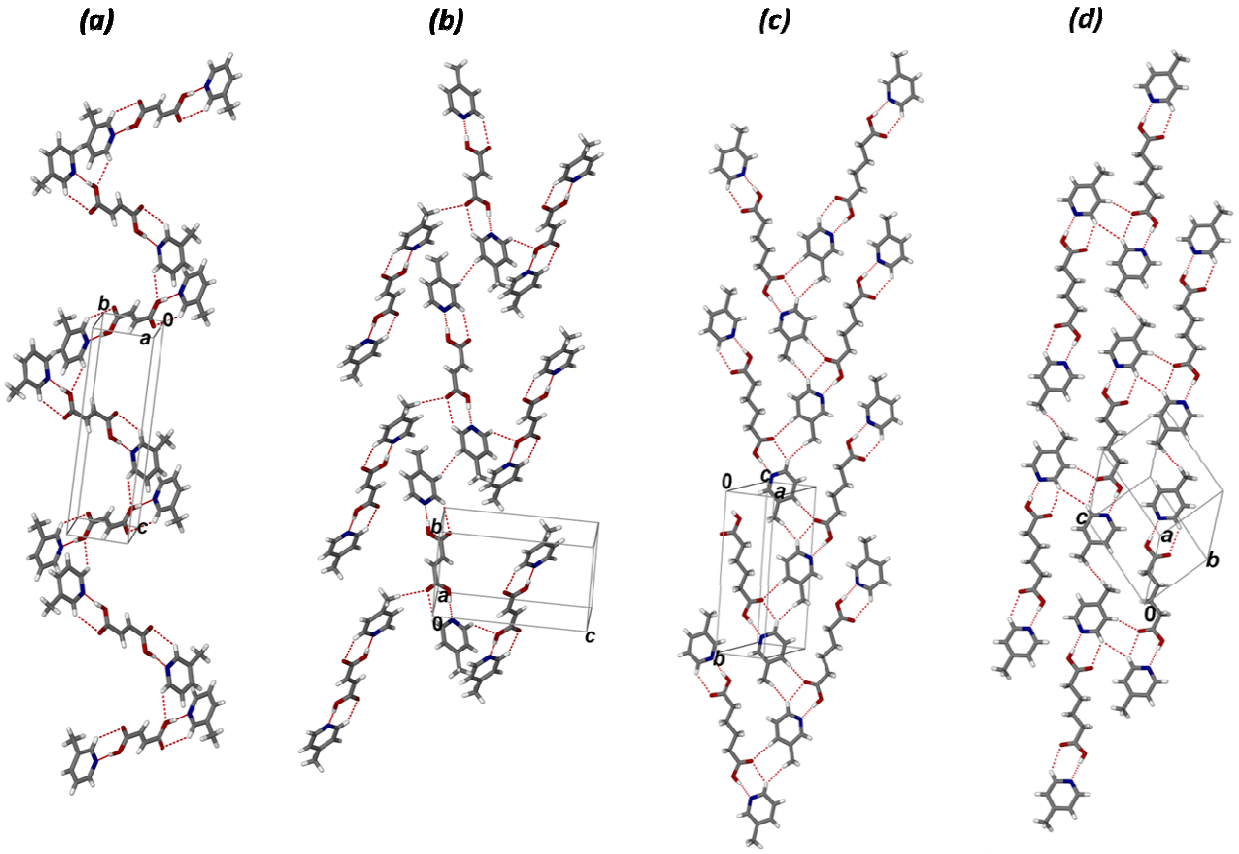

Fig. 2 The hydrogen bonded networks in (a) **FUM3PIC**, (b) **FUM4PIC**, (c) **ADI3PIC** and (d) **ADI4PIC**

The **ADI4PIC** structure also consists of 2D sheets formed as a result of five short contacts in the *bc* plane (C2–H2•••O17; 3.376(5) Å; 142.9°, C19–H19•••O8; 3.370(4) Å; 143.6°, C5–H5•••O16; 3.307(5) Å; 153.6°, C22–H22•••O10; 3.317(6) Å; 154.5° and H24C•••H7C = 2.21 Å). The 2D sheets interact with neighbouring sheets via two C–H•••π interactions involving two of the adipic acid hydrogen atoms (H14B and H11B) and the picolinyl ring (CH•••π = 2.781 Å and 2.763 Å) (Fig. 2(d)).

Melting point, solubility and Hirshfeld surface analysis

The solubilities of the four solvates as well as the previously reported **FUMDABCO** (CCDC code HUSTAQ[21]), **ADIDABCO** (UNEFOI[23]), **FUM** (FUMAAC[40]) and **ADI** (ADIPAC13[41]) were measured in water and ethanol and the values are given in Table 3. Their melting points were determined using DSC (Table 3) and the DSC thermograms are presented in the ESI (Fig. S7 and S8). Both melting point and solubility are influenced by intermolecular interactions and are related via the enthalpy of fusion.[42] Generally, compounds with strong intermolecular interactions have high melting points and high heat of fusion and conversely low solubilities.[42] The melting points of the multicomponent crystals are lower than the corresponding dicarboxylic acid and they follow the order

FUM>FUMDABCO>FUM3PIC>FUM4PIC

and

ADI>ADIDABCO>ADI3PIC>ADI4PIC

These trends are attributed to the appearance of the stronger intermolecular interactions (hydrogen bond, charge assisted hydrogen bond) in the multicomponent crystals. The carboxylic acid homo dimers in the pure acids are stronger than the charge assisted heterosynthons in the salts which are, in turn, stronger than the acid•••picoline heterosynthons in the solvates. The aqueous solubility in both series does not follow the expected trend but rather follows the order

FUM3PIC<FUM<FUMDABCO<FUM4PIC

and

ADI3PIC<ADI<ADIDABCO<ADI4PIC

We found no correlation between the ethanol solubility and the melting points for both the **FUM** and **ADI** series. It is interesting to note that in both series, the solvates containing 3-picoline show a somewhat different behaviour and have the lowest aqueous solubilities. In order to understand how the melting point and the solubility relate to the supramolecular structure, 2D fingerprint plots were generated using CrystalExplorer[30,31] which gave a breakdown of the intermolecular interactions as well as their contributions to the total Hirshfeld surface (Table 3). For the structures **FUM3PIC**, **FUM4PIC**, **ADI3PIC** and **ADI4PIC**, each fragment was defined as a whole supramolecular unit consisting of two 3- or 4-picoline molecules hydrogen bonded to a dicarboxylic acid. Following the same logic, **FUMDABCO** and **ADIDABCO** fragments were also taken to be two **DABCO** molecules and one dicarboxylic acid (Fig. S9). The contributions from the H•••H, O•••H and C•••H interactions were plotted with the aqueous solubilities and melting points as depicted in Fig. 3.

In both the **FUM** and **ADI** series, generally, the O•••H interactions correlate with the melting point and the highest O•••H contribution being observed in the compound with the highest melting point. On the other hand, there is a general increase of the H•••H interactions with decreasing melting point. Interestingly, C•••H interactions in both the **FUM** and the **ADI** series show an inverse relationship to the solubility. When considering the solvates only (Fig. 4), the C•••H interactions, which are considered to be attractive, contribute more in **FUM3PIC** and **ADI3PIC** than in **FUM4PIC** and **ADI4PIC**, while the H•••H interactions which are somewhat an indicator of an unfavoured packing feature contribute more in the **FUM4PIC** and **ADI4PIC**. A closer inspection of the 2D fingerprint plots of the **FUM3PIC** and **FUM4PIC** reveals that the closest atom–atom contact for the H•••H interactions obtained by taking the sum of *de* and *di* at the point of the spike is shorter in **FUM4PIC** (2.13 Å) and **ADI4PIC** (2.04 Å) than in **FUM3PIC** (2.40 Å) and **ADI3PIC** (2.12 Å). This indicates a more efficient packing with better balanced interactions in the **FUM3PIC** and **ADI3PIC** structures than in the **FUM4PIC** and **ADI4PIC**. The close packing in these structures as well as the higher percentage of the C•••H attractive interactions are contributing to their lower solubilities.

Table 3 Melting point (Mp), solubility (aqueous (*S*w) and ethanol (*S*e)), H•••H, O•••H and C•••H contributions for the multicomponent crystals and the pure acids

Compound	Mp (°C)	*S*w (mg/ml)	*S*e (mg/ml)	H•••H (%)	O•••H (%)	C•••H (%)
FUM	279	42	35	12.3	53.0	13.7
FUMDABCO	190	95	305	39.6	49.6	6.8
FUM3PIC	69	35	15	47.5	22.1	20.3
FUM4PIC	66	136	271	50.0	23.3	16.0
ADI	151	138	89.0	43.5	45.9	4.6
ADIDABCO	136	156	30.0	63.7	32.5	2.6
ADI3PIC	57	19	148	55.4	21.5	17.8
ADI4PIC	49	252	20	56.8	19.9	13.8

Conclusions

In summary, six multicomponent crystals involving fumaric acid and adipic acid were synthesised and the relationships of the supramolecular structures with the melting points and solubilities were discussed. The structures are very similar in that the supramolecular units formed by the acid-base pairs are connected primarily via strong O–H•••N hydrogen bonds. Secondary interactions such as H•••H, CH•••O, π•••π and CH•••π are utilised in the packing. The melting point showed partial correlation with the aqueous solubility but no correlation with ethanol solubility. Analysis of the crystal structures using CrystalExplorer provided a breakdown of the intermolecular interactions and it was found that the O•••H interactions correlate with the melting point; a decrease in melting point corresponds to a decrease in O•••H interactions while the C•••H interactions show an inverse relationship to the aqueous solubility.

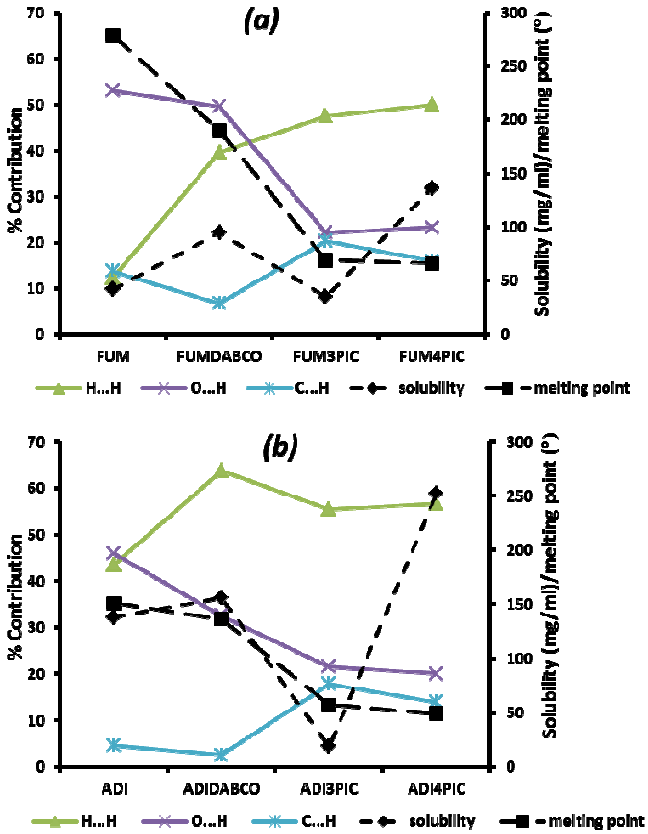

Fig. 3 Plots of the melting point, aqueous solubility and the percentage contributions from H•••H, O•••H and C•••H interactions in the **FUM** series (a) and in the **ADI** series (b)

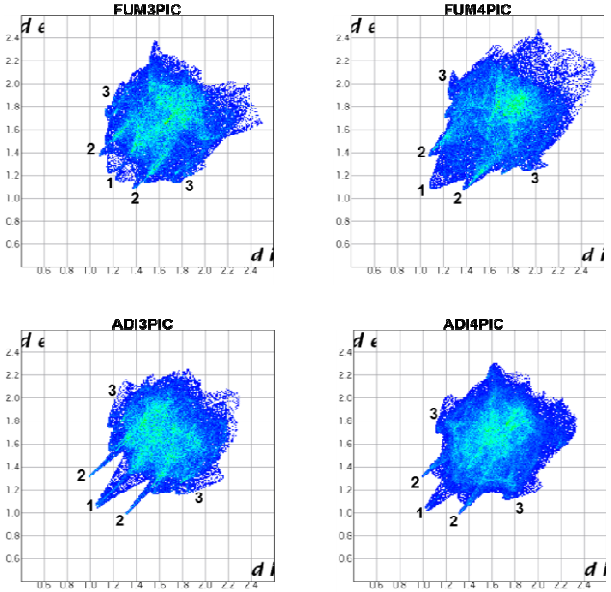

Fig. 4 The 2D plots derived from Hirshfeld surface analysis for **FUM3PIC**, **FUM4PIC**, **ADI3PIC** and **ADI4PIC**. Spikes labelled **1-3** represent the H•••H, O•••H and C•••H interactions respectively

Acknowledgements

We would like to thank the National Research Foundation of South Africa and the Cape Peninsula University of Technology for financial assistance.

References

Crystal Engineering Research Unit, Department of Chemistry, Cape Peninsula University of Technology, P. O. Box 652, Cape Town, South Africa, 8000. E-mail: bathorin@cput.ac.za; Fax: +27 21 460 3854; Tel: +27 21 460 8354

[1] A. Newman and N. Schultheiss, *Cryst. Growth Des.*, 2009, **9**, 2950-2967
[2] W. Jones, S. W. D. Motherwell and A. V. Trask, *MRS Bull.*, 2006, **31**, 875-879
[3] A. Delori, T. Friščić and W. Jones, *CrystEngComm*, 2012, **14**, 2350-2362
[4] C. B. Aakeröy, S. Forbes and J. Desper, *CrystEngComm*, 2014, DOI: 10.1039/c4ce00206g
[5] N. R. Goud, R. A. Khan and A. Nangia, *CrystEngComm*, DOI: 10.1039/c4ce00103f
[6] A. T. M. Serajuddin, *Adv. Drug Delivery Rev.*, 2007, **59**, 603-616
[7] N. Blagden, M. De Matas, P. T. Gavan and P. York, *Adv. Drug Delivery Rev.*, 2007, **59**, 617-630
[8] A. V. Trask, S. W. D. Motherwell and W. Jones, *Cryst. Growth Des.*, 2005, **5**, 1013-1021
[9] *Pharmaceutical Salts and Co-crystals*, ed, J. Wouters, L. Quere, D. E. Thurston, Royal Society of Chemistry, 2011
[10] T. Takagi, C. Ramachandran, M. Bermejo, S. Yamashita, L. X. Yu and G. L. Amidon, *Mol. Pharm.,* 2006, **3**, 631-643
[11] A. R. Katritzky, R. Jain, A. Lomaka, R. Petrukhin, U. Maran and M. Karelson, *Cryst. Growth Des.*, 2001, **1**, 261-265
[12] W. L. Jorgensen and E. M. Duffy, *Adv. Drug Delivery Rev.,* 2002, **54**, 355-366
[13] S. J. Delaney, *Drug Discov Today Biosilico,* 2005, **10**, 289-295
[14] B. E. Mitchell and P. C. Jurs, *J. Chem. Inf. Comput. Sci.*, 1998, **38**, 489-496
[15] J. Huuskonen, *J. Chem. Inf. Comput. Sci.,* 2000, **40**, 773-777
[16] L. D. Hughes, D. S. Palmer, F. Nigsch and J. B. O. Mitchell, *J. Chem. Inf. Model.*, 2008, **48**, 220-232
[17] S. H. Yalkowsky and S. C. Valvani, *J. Pharm. Sci.*, 1980, **69**, 912-922
[18] M. K. Stanton, S. Tufekcic, C. Morgan and A. Bak, *Cryst. Growth Des.*, 2009, **9**, 1344-1352
[19] C. B. Aakeröy, S. Forbes and J. Desper, *J. Am. Chem. Soc.*, 2009, **131**, 17048-17049
[20] D. J. Good and N. Rodriguez-Hornedo, *Cryst. Growth Des.,* 2009, **9**, 2252-2264
[21] K. F. Bowes, G. Ferguson, A. J. Lough and C. Glidewell, *Acta Crystallogr. Sect. B:Struct. Sci.*, 2003, **59**, 100-117
[22] R. Gobetto, C. Nervi, M. R. Chierotti, D. Braga, L. Maini, F. Grepioni, R. K. Harris and P. Hodgkinson., *Chem. Eur. J.*, 2005, **11**, 7461-7471
[23] D. Braga, L. Maini, G. de Sanctis, K. Rubini, F. Grepioni, M. R. Chierotti and R. Gobetto, *Chem. Eur. J.*, 2003, **9**, 5538-5548
[24] A. J. Cruz-Cabeza, *CrystEngComm*, 2012, **14**, 6362-6365
[25] Calculator plugins were used for the structure property prediction and calculation, Marvin 6.3.0, 2014, ChemAxon (http://www.chemaxon.com)
[26] P. Gilli, L. Pretto, V. Bertolasi and G. Gilli, *Acc. Chem. Res.*, 2009, **42**, 32-44
[27] B. R. Bhogala, S. Basavoju and A. Nangia, *CrystEngComm,* 2005, **7**, 551-562
[28] G. Ramon, K. Davies and L. R. Nassimbeni, *CrystEngComm,* 2014, DOI: 10.1039/c3ce41963k
[29] U. Domannska, A. Pobudkowska, A. Pelczarska and P. Gierycz, *J. Phys. Chem. B*, 2009, **113**, 8941-8947
[30] M. A. Spackman and D. Jayatilaka, *CrystEngComm*, 2009, **11**, 19-32
[31] J. J. McKinnon, D. Jayatilaka and M. A. Spackman, *Chem. Commun.*, 2007, 3814-3816
[32] Mercury CSD 2.0 - New Features for the Visualization and Investigation of Crystal Structures, C. F. Macrae, I. J. Bruno, J. A. Chisholm, P. R. Edgington, P. McCabe, E. Pidcock, L. Rodriguez-Monge, R. Taylor, J. van de Streek and P. A. Wood, *J. Appl. Cryst.*, 2008, **41**, 466-470
[33] COLLECT Data Collection Software (1999) Nonius, Delft, The Netherlands
[34] Z. Otwinowski and W Minor, Processing of X-ray diffraction data collected in oscillation mode. Methods in enzymology, *Macromolecular Crystallography, part A*, 1997, **276**, 307-326
[35] Bruker 2005, *APEX2*, Version 1.0-27. Bruker AXS Inc., Madison, Wisconsin, USA
[36] Bruker 2004, *SAINT-Plus* (including *XPREP*), Version 7.12. Bruker AXS Inc., Madison, Wisconsin
[37] Bruker 2003, *XPREP2*, Version 6.14. Bruker AXS Inc., Madison, Wisconsin, USA
[38] G. M. Sheldrick, *SHELXS-97* and *SHELXL-97* programs for crystal structure determination and refinement, 1997, University of Gottingen, Germany
[39] L. J. Barbour, *J. Supramol. Chem.*, 2001, **1**, 189-191
[40] C. J. Brown, *Acta Crystallogr.*, 1966, **21**, 1-5
[41] A. Gunay, K. H. Theopold and G. P. A. Yap, *Private Communication,* 2008, CCDC 691169
[42] M. E. Aulton, *Pharmaceutics: The science of dosage form design*, Elsevier Limited, 2002